#8

ORIGINAL CONTRIBUTION

Regional Distribution of Sodium-Dependent Excitatory Amino Acid Transporters in Rat Spinal Cord

Susan A. Queen, PhD, PT[1;2]; J. Patrick Kesslak, PhD[3]; Richard J. Bridges, PhD[4]

[1]Department of Orthopedics and Rehabilitation and Neurosciences, University of New Mexico, Albuquerque, New Mexico; [2]University of Kentucky, Lexington, Kentucky; [3]Institute for Brain Aging, University of California Irvine; [4]Center for Structural and Functional Neuroscience, University of Montana, Missoula, Montana

Received February 22, 2006; accepted November 13, 2006

Abstract

Background/Objective: The excitatory amino acid transporters (EAATs), or sodium-dependent glutamate transporters, provide the primary mechanism for glutamate removal from the synaptic cleft. EAAT distribution has been determined in the rat brain, but it is only partially characterized in the spinal cord.

Methods: The regional anatomic distribution of EAATs in spinal cord was assessed by radioligand autoradiography throughout cervical, thoracic, and lumbar cord levels in female Sprague-Dawley rats. EAAT subtype regional distribution was evaluated by inclusion of pharmacologic transport inhibitors in the autoradiography assays and by immunohistochemistry using subtype-specific polyclonal antibodies to rat GLT1 (EAAT2), GLAST (EAAT1), and EAAC1 (EAAT3) rat transporter subtypes.

Results: [^{3}H]-D-Aspartate binding was distributed throughout gray matter at the 3 spinal cord levels, with negligible binding in white matter. Inclusion of pharmacologic transport inhibitors indicates that the EAAT2/GLT1 subtype represents 21% to 40% of binding. Both EAAT1/GLAST and EAAT3/EAAC1 contributed the remainder of binding. Immunoreactivity to subtype-specific antibodies varied, depending on cord level, and was present in both gray and white matter. All 3 subtypes displayed prominent immunoreactivity in the dorsal horn. EAAT3/EAAC1 and to a lesser extent EAAT1/GLAST immunoreactivity also occurred in a punctate pattern in the ventral horn.

Conclusions: The results indicate heterogeneity of EAAT distribution among spinal cord levels and regions. The presence of these transporters throughout rat spinal cord suggests the importance of their contributions to spinal cord function.

J Spinal Cord Med. 2007;30:263–271

Key Words: Spinal cord; Glutamate plasma membrane proteins; Autoradiography; Immunohistochemistry; Amino acid transporters, Excitatory

INTRODUCTION

As the major excitatory amino acid in the spinal cord, glutamate contributes to sensory signaling in the dorsal horn (1), motor signaling in ventral horn cells (2), and gray and white matter pathophysiology (3,4). Under normal conditions, the excitatory amino acid transporters (EAATs) tightly regulate extracellular glutamate at low micromolar resting concentrations via rapid, sodium (Na^+)-dependent uptake against millimolar intracellular tissue concentrations (5,6). The importance of EAATs in spinal cord is evidenced by their contribution to the neuropathology of amyotrophic lateral sclerosis (7–9), acute spinal cord injury (10,11), traumatic brain injury (12), and pain (13). These pathologies are suggested to occur either by reduced uptake and/or reversal of Na^+-dependent glutamate transport (7,10–12,14,15).

The EAAT system is best characterized in brain tissue. Na^+-dependent glutamate transporters recognize L-glutamate, L-aspartate, or D-aspartate as substrates (16,17). Initial kinetic and pharmacologic data implied the existence of subtypes (see Robinson and Dowd [18] for review). Autoradiography with [^{3}H]-D-aspartate (19)

Please address correspondence to Susan A. Queen, Physical Therapy Program, Health Sciences Center MSC09 5230, University of New Mexico, Albuquerque, NM 87131-0001; phone: 505.272.5451; fax: 505.272.8079 (e-mail: squeen@salud.unm.edu).

This work was supported in part by grants from NINDS NS387903 (SAQ), NS30570 (RJB), and the Paralysis Project of America (SAQ). Portions of this study were presented at the Society for Neurosciences annual meetings in 2001 and 2003.

or [^{3}H]-L-aspartate (20,21) indicated distinct distribution patterns of Na^+-dependent transport in rat brain, which were consistent with later immunohistochemistry and in situ hybridization studies in a number of mammalian species, including humans (22–25). Cloning identified 5 subtypes within a distinct gene family in mammalian species, designated EAAT1 through EAAT5 (see Danbolt [26] for review). EAAT1, EAAT2, and EAAT3 are highly homologous to the rat genes GLAST, GLT1, and EAAC1, respectively (27). Astrocytes in brain predominantly express EAAT1/GLAST and EAAT2/GLT1 proteins, and neurons predominantly express EAAT3/EAAC1 (23). Increased complexity of the EAAT system is evidenced by (a) the presence of EAAT2/GLT1 splice variants in cortical neurons (12,28–31), and (b) the apparent expression of only EAAT3/EAAC1 mRNA and protein by oligodendroglia (28). The majority of glutamate transport in brain is attributed to EAAT2/GLT1, the most abundant of the EAATs in many brain regions (32). EAAT4 appears to be located primarily in cerebellum (33), and EAAT5 (34) is limited to retina cells.

Characterization of the distribution of the Na^+-dependent transporters in adult rat spinal cord consists of immunodetection of protein in naïve cervical cord (22–25) and injured thoracic cord (35) and nonradioactive in situ hybridization in naïve cervical cord (25,28). To our knowledge, the regional distribution of Na^+-dependent [^{3}H]-D-aspartate binding has not been reported in rat spinal cord. Such characterization will be instrumental to accurately assess the effect of spinal cord injury on the transporter system.

In this paper we report on the regional distribution of Na^+-dependent transporters throughout the cervical, thoracic, and lumbar naïve rat spinal cord using radioligand autoradiography in tissue sections. Regional EAAT subtype distribution was determined in part by the inclusion of subtype-selective transport inhibitors in radioligand binding assays and by antibody-specific binding with immunohistochemistry (IHC). Autoradiography and IHC provide complementary information. Radioligands bind to the active uptake site and are therefore apt to indicate functional protein, while antibody binding to C- or N-protein terminals indicates the presence of protein but not necessarily functional transporter. Autoradiography also permits quantification of binding site densities, whereas immunohistochemistry provides superior regional resolution and improved subtype delineation compared to autoradiography. EAATs bind as well as transport glutamate in the synaptic cleft. Therefore, the extent to which they shape the postsynaptic signal and protect tissue from excitotoxic damage is hypothesized to be reflected by the density of transporters in close proximity to receptors (36–39), which emphasizes the importance of quantifying transporter density.

MATERIALS AND METHODS

[^{3}H]-D-aspartate was purchased from Dupont NEN (666 GBq/mmol) (Boston, MA). Excitatory amino acid agonists and EAAT transport inhibitors were obtained from Tocris Cookson (Ellisville, MO) or contributed by one of the authors (RJB) (L-*trans*-2,3-pyrrolidine dicarboxylate). The polyclonal EAAC1, GLT1, and GLAST antibodies were obtained from Chemicon International (Temecula, CA); secondary antibodies and sera (biotinylated rabbit anti–goat and goat anti–rabbit sera, normal goat or rabbit serum) and Vectastain ABC kit were from Vector Laboratories (Burlingame, CA). All other chemicals were purchased from Sigma Chemical (St Louis, MO).

Autoradiography with [^{3}H]-D-Aspartate

Autoradiography with [^{3}H]-D-aspartate was based on the method of Anderson et al (19). Eight female Sprague-Dawley rats (Harlan, Indianapolis, IN), 220 to 250 g, were housed in 12:12 light/dark conditions. The University of Kentucky Institutional Animal Care and Use Committee approved all animal care and usage, in accordance with the requirements of the Association for Assessment and Accreditation of Laboratory Animal Care. Animals were sacrificed by rapid decapitation without anesthesia, and the spinal column was quickly removed and chilled in ice for 20 minutes prior to cord removal. Cervical, thoracic, and lumbar regions were identified and separated, and each piece was frozen on powdered dry ice prior to storage at −76°C until sectioned. Eight-micron cryostat cross sections were thaw mounted onto chrome alum gelatin-coated glass slides. Duplicate cross sections were taken through the spinal cord at the approximate levels of C4, C6, T3, T5, T8, T10, L1, and L3, with a section stained with Nissl at the beginning of each level.

Assay. Slides were warmed from −76°C to room temperature for 5 minutes before pretreatment at 30°C in xylene (10 minutes) to minimize radioligand sequestration in lipid vesicles, followed by preincubation in 50-mmol/L Tris hydrochloride with 300-mmol/L sodium chloride, pH 7.4 (10 minutes), to remove endogenous amino acids and ions. This step would also remove any excessive glutamate that might have accumulated following rapid decapitation. Sections were then incubated at 0°C to 2°C for 10 minutes with 100 nmol/L [^{3}H]-D-aspartate (666 GBq/mmol). The Na^+-dependent transport inhibitors dihydrokainate (DHK, 100 μmol/L), L-*trans*-2,4-pyrrolidine dicarboxylate (2,4-PDC, 500 μmol/L), or L-*trans*-2,3-pyrrolidine dicarboxylate (2,3-PDC, 100 μmol/L) were added to characterize transporter subtype. To eliminate possible binding to excitatory amino acid receptors, 100 μmol/L each of N-methyl-D-aspartate (NMDA), 1S,3R-trans ACPD (tACPD), kainate (KA), and AMPA were added to the incubation. Nonspecific binding was determined by addition of 100-μmol/L D,L-β-*threo*-hydroxyaspartate. Unbound radioligand was removed by dipping slides sequentially into a series of 4 containers of ice-cold buffer within 30

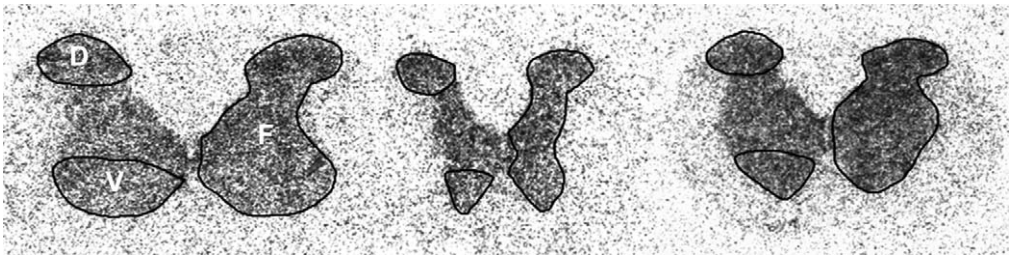

Figure 1. Representative autoradiograms of ^{3}H-D-aspartate binding in 8-μm tissue sections from naïve Sprague-Dawley rats from *(left to right)* cervical, thoracic, and lumbar cord levels. Circumscribed areas on the left half of the gray matter indicate the dorsal (D) and ventral (V) regions analyzed; those on the right indicate "full" (F) gray matter measures. Note the slightly higher density in dorsal than ventral regions in cervical and lumbar compared to thoracic spinal cord.

seconds. Sections were rapidly air dried and vacuum desiccated overnight prior to loading into x-ray cassettes. Tissue sections and a methylacrylate standard (Amersham) were exposed to tritium-sensitive Hyperfilm (Amersham, Piscataway, NJ) for 9 weeks at 4°C.

Data Analysis. Specific binding was quantitated by densitometric analysis using the public-domain software NIH Image (developed at the US National Institutes of Health and available at http://rsb.info.nih.gov/nih-image). Spinal gray matter was analyzed in the regions indicated in Figure 1, with measures taken bilaterally from the dorsal horns, ventral horns, and a "full" measure of total gray matter. Right and left measures were averaged prior to conversion to fmol/mg protein values based on the radioligand-specific activity of 666 GBq/mmol. Duplicate tissue slices were analyzed from each of the 8 cord levels per animal. Quantitative data within each individual region (cervical, thoracic, or lumbar) were averaged because of the consistency of the data within each animal.

Immunohistochemistry

Transporter subtype specificity was also determined by incubation of 10-μm tissue cross sections with primary polyclonal, carboxy-terminus antibodies to the rat isoforms EAAC1 (EAAT3), GLT1 (EAAT2), or GLAST (EAAT1). Duplicate sections were taken sequentially after those collected for autoradiography at the same spinal cord levels. Tissue was stored at −76°C until assayed. All incubations were done at room temperature in 50 mmol/L Tris buffer (Tris), pH 7.4, unless otherwise indicated. Tissue was rinsed for 5 minutes each in Tris and Tris/0.5% bovine serum albumin between all assay steps. Tissue was post-fixed for 5 minutes in 4% paraformaldehyde and pretreated in 3% hydrogen peroxide prior to blocking for 20 minutes in 4% normal goat (GLT1 or GLAST) or normal rabbit (EAAC1) serum. Primary antibody (EAAC1, 1:8,000; GLT1, 1:3,000; or GLAST, 1:5,000) was applied for 24 hours at 4°C followed by secondary antibody (biotinylated goat anti-rabbit immunoglobulin G (IgG) for GLT1 or GLAST, or rabbit anti-goat for EAAC1, at 1:400) for 1 hour. Avidin-biotin (Vectastain ABC Kit, Vector Laboratories; 1:200) was applied and antibody binding visualized with diaminobenzidine with hydrogen peroxide.

Controls consisted of normal goat or rabbit IgG replacing the transporter primary antibodies. No specific binding occurred in the absence of primary antibody. Sections were visualized by light microscopy, and Rexed laminae were identified based on the descriptions of Molander et al (40,41).

Statistical Analysis

Specific binding density of [^{3}H]-D-aspartate between cord regions and cord levels was compared by 1-way analysis of variance (ANOVA) with InStat 3.0 (San Diego, CA). The effect of the inhibitors on [^{3}H]-D-aspartate binding was converted to percent of total binding in the absence of inhibitor for each region analyzed. Statistical comparison of the normalized data was by 1-way ANOVA with the Dunnet post hoc analysis.

RESULTS

Autoradiography

It is important to note that autoradiography measures the density of a bound radioligand. In these experiments, [^{3}H]-D-aspartate was used to measure density of Na^+-dependent glutamate transporters. Incubation in a sodium-free assay buffer containing 300-mmol/L choline chloride completely eliminated [^{3}H]-D-aspartate binding in spinal cord tissue slices, as did the addition of 100 μmol/L D,L-β-*threo*-hydroxyaspartic acid (data not shown). These results confirm the dependence of binding on Na^+ ions and indicate that all [^{3}H]-D-aspartate binding represents specific binding. In the presence of sodium, [^{3}H]-D-aspartate binding was uniform throughout gray matter in cervical, thoracic, and lumbar spinal cord in dorsal, intermediate, and ventral cord laminae, indicating a consistent distribution of Na^+-dependent glutamate transporters in spinal cord gray matter (Figure 1).

In contrast to the obvious radioligand binding throughout gray matter, binding in white matter was negligible and not consistently measurable above back-

Table 1. Mean (± SE) Specific Binding of ^{3}H-D-Aspartate to EAAT Sites in Rat Spinal Cord (fmol/mg Protein)

Cord Region	Cervical	Thoracic	Lumbar
Dorsal Laminae	275.76 ± 69.07	273.66 ± 44.26	296.81 ± 48.44
Ventral Laminae	246.25 ± 66.22	268.03 ± 43.69	251.11 ± 20.70
Full Gray	255.76 ± 69.03	270.76 ± 43.31	283.40 ± 49.69

Values represent average of bilateral measures from duplicate slices at 2 cervical levels, 4 thoracic levels, and 2 lumbar levels from 8 rats. Dorsal laminae, ventral laminae, and full gray were measured as depicted in Figure 1. Note the slightly greater density in dorsal than ventral regions and in cervical lumbar compared to thoracic spinal cord, although means are not significantly different.

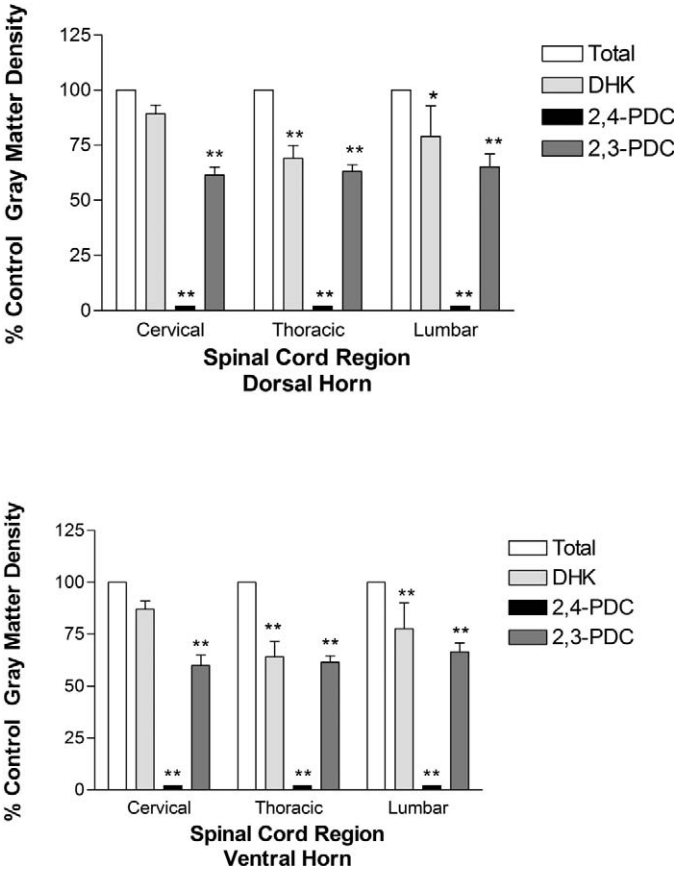

Figure 2. Pharmacologic differentiation of glutamate transporter subtypes in Sprague-Dawley spinal cord by inclusion of transport inhibitors in autoradiographic assays. Inhibitors were included at 10 times their Km or Ki values for uptake in other expression systems (DHK, 100 μmol/L; 2,4-PDC, 500 μmol/L; 2,3-PDC, 100 μmol/L). Binding density was quantitated bilaterally in each section and then averaged from duplicate sections at 2 cervical (C4, C6), 4 thoracic (T3, T5, T8, T10), and 2 lumbar levels (L1, L3) from each rat—from 6 rats for DHK and from 12 to 15 rats for 2,4-PDC and 2,3-PDC. Inhibitor binding is represented as the percent of total binding for each region analyzed. * = P, 0.05; ** = $P <$ 0.01 compared to control.

ground. In the absence of all receptor agonists, binding increased by an average of 60% in gray matter measures, with modest binding apparent in white matter, indicative of the ability of [^{3}H]-D-aspartate to bind to spinal cord glutamate receptors. Xylene pretreatment decreased binding density by approximately 40% but did not change the [^{3}H]-D-aspartate distribution pattern (data not shown), which indicates a uniform response to the preincubation step throughout spinal cord.

Means of [^{3}H]-D-aspartate binding did not differ significantly between cord levels or regions within cord levels (Table 1). Slightly higher binding densities occurred in the dorsal compared to the ventral horn at the cervical and lumbar cord levels within gray matter (Table 1), with no apparent focal areas of increased binding in the ventral horn that would correspond to motor neurons (Figure 1).

Inclusion of glutamate transport inhibitors variably affected [^{3}H]-D-aspartate binding in spinal cord gray matter (Figure 2). The transportable substrate inhibitor 2,4-PDC (500 μmol/L), which appears potent enough to inhibit all 3 rat transporters at the concentration employed (27), abolished binding in all cord levels and regions. Conversely, variable effects were produced with the nontransportable inhibitors 2,3-PDC and DHK, both of which more potently inhibit EAAT2/GLT1 than EAAT1/GLAST or EAAT3/EAAC1 (42). Inclusion of 2,3-PDC decreased binding density in dorsal and ventral laminae at all 3 cord levels by approximately 34% to 40% ($P <$ 0.01) compared to control levels. In contrast, DHK reduced binding by 31% to 36% ($P < 0.01$) in thoracic dorsal and ventral regions and by 21% ($P < 0.05$) and 23% ($P < 0.01$) in lumbar dorsal and ventral cord, but by only 11% and 13% in cervical dorsal and ventral gray matter, respectively. No apparent dorsal/ventral regional specificity occurred with the different inhibitors tested.

Immunohistochemistry

The EAAT1/GLAST, EAAT2/GLT1, and EAAT3/EAAC1 Na^+-dependent glutamate transporters each displayed unique regional distribution patterns that varied moderately among the 3 levels of rat spinal cord gray matter (Figure 3). Immunohistochemistry defined intense binding in the dorsal horn particularly at the cervical and thoracic cord levels (A, B, D, E, G, H; see Molander et al [40,41] for

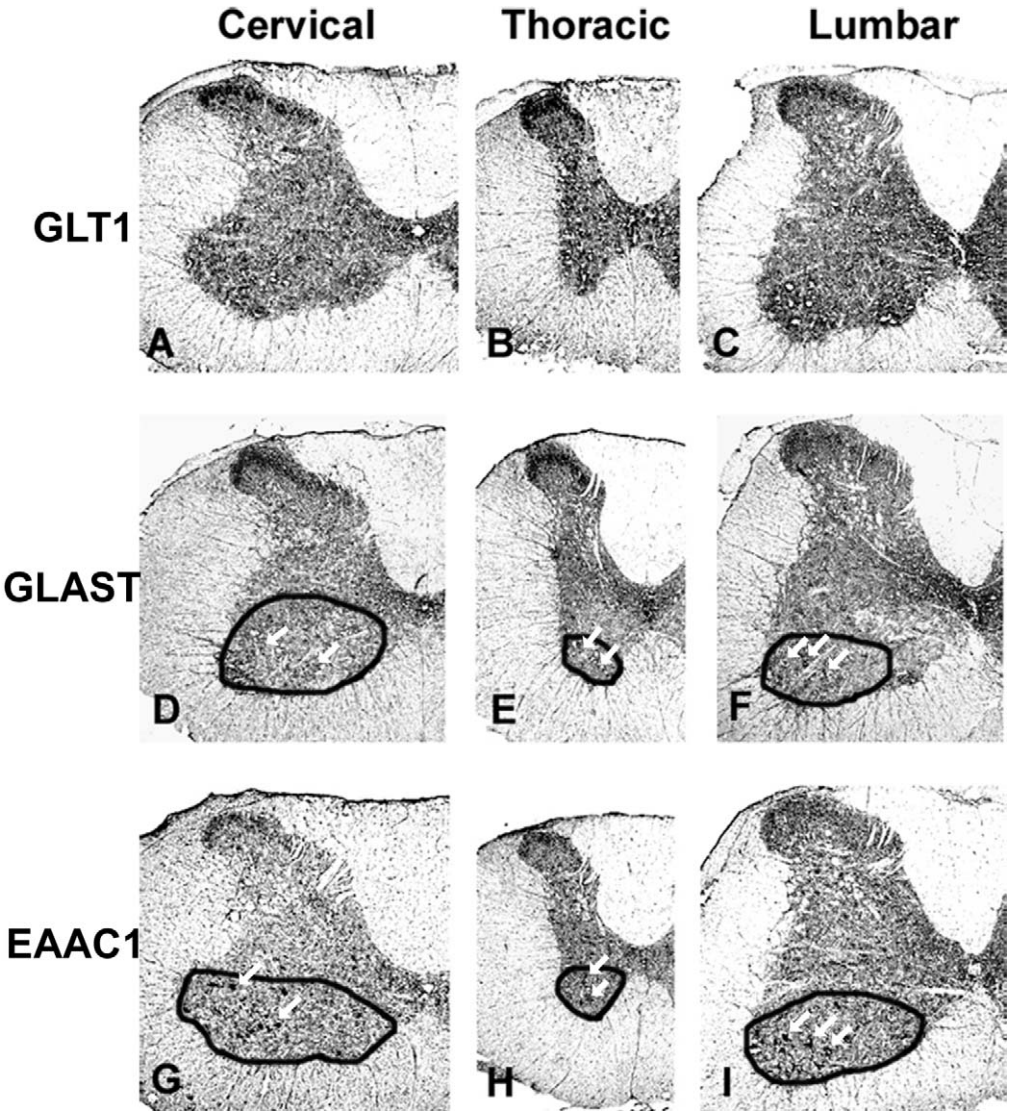

Figure 3. Spinal cord glutamate transporter subtype regional distribution in Sprague-Dawley rats as determined by immunohistochemical detection of EAAT2/GLT1 (A, B, C), EAAT1/GLAST (D, E, F), and EAAT3/EAAC1 (G, H, I) in cervical (A, D, G), thoracic (B, E, H), and lumbar (C, F, I) cord. Duplicate, 10-μm spinal cord cryostat cross sections (post-fixed with paraformaldehyde) were incubated with primary antibodies to GLT1 (1:3,000), GLAST (1:5,000), or EAAC1 (1:8,000). Immunoreactivity was greatest in gray compared to white matter. All 3 transporter subtypes were expressed heavily in the dorsal horn, particularly in cervical and thoracic sections. Dorsal horn binding intensity was greatest in with EAAT2/GLT1 and EAAT1/GLAST in laminae II (A–F). Dorsal horn EAAT3/EAAC1 immunoreactivity, which was less intense than that of EAAT2/GLT1 and EAAT1/GLAST, included laminae I at all 3 cord levels (G,H,I) and laminae III at the lumbar level (I). EAAT2/GLT immunoreactivity was moderately intense in other cord laminae. EAAT3/EAAC1 immunoreactivity was also characterized by a punctate pattern in the ventral horn, which was most pronounced at the cervical (G) and lumbar (I) cord levels. EAAT1/GLAST immunoreactivity produced a less intense punctate pattern in the ventral horn (D, E, F). Antibodies to all 3 rat glutamate transporter subtypes produced a radial pattern of immunoreactivity in white matter. Images were visualized at 4×. The arrows within circumscribed regions highlight the punctate immunoreactivity with EAAT1/GLAST (D, E, F) and EAAT3/EAAC1 (G, H, I).

description of spinal cord anatomy). Of the 3, EAAT2/GLT1 (Figure 3, C) retained prominent immunoreactivity in the lumbar dorsal horn. Immunoreactivity for EAAT1/GLAST (Figure 3, D–F) and EAAT2/GLT1 (Figure 3, A and B) was most distinct in Rexed lamina II, whereas the EAAT3/EAAT1 (Figure 3, G–I) immunoreactivity pattern included laminae I at the cervical and thoracic levels, with light immunoreactivity also present in laminae III at the lumbar level (Figure 3, I). EAAT3/EAAC1 produced a pronounced (Figure 3, G and I), and EAAT1/GLAST a light (Figure 3, D and F), punctate pattern of immunoreactivity in the ventral horn, which appears to correspond to motor

nuclei based on comparison with Nissl stain. Immunoreactivity with EAAT1/GLAST was also evident in laminae X, particularly at the lumbar cord level. Immunoreactivity throughout other cord regions appeared uniform for each EAAT subtype. A radial pattern of light immunoreactivity in white matter was evident with all 3 antibodies.

DISCUSSION

The presence and function of EAAT proteins and mRNA in rat spinal cord tissue was previously confirmed. We now provide an autoradiographic depiction of regional EAAT distribution and compare transporter distribution at cervical, thoracic, and lumbar cord levels with autoradiography and immunohistochemistry.

Autoradiography with [^{3}H]-D-aspartate indicated a generalized distribution of the Na^+-dependent glutamate transporters throughout gray matter at cervical, thoracic, and lumbar levels in all regions, with no statistically significant differences in quantitative binding density (Table 1). Only negligible binding was present in white matter. That the glutamate transport inhibitors 2,3-PDC and DHK collectively inhibited [^{3}H]-D-aspartate binding by 11% to 40%, depending on cord level and region (Figure 2), suggests that the EAAT2/GLT1 subtype accounts for up to 40% of Na^+-dependent transporter distribution in dorsal and ventral cord regions. The low density of Na^+-dependent transporters, coupled with the weak beta emissions of the tritium radioligand (43), necessitated a prolonged exposure time. These factors likely accounted for the low autoradiographic resolution in the present study.

Immunohistochemistry provided superior resolution to specify gray matter heterogeneity at cervical, thoracic, and lumbar cord levels (Figure 3). Antibodies to EAAT3/EAAC1, EAAT2/GLT1, and EAAT1/GLAST revealed a greater intensity of EAAT subtype binding in dorsal horn gray matter. The EAAT3/EAAC1 antibody strongly labeled the ventral horn in a motor neuronal distribution, with a similar but lighter immunoreactivity pattern produced by the EAAT1/GLAST antibody (Figure 3, D, F, G, and I). Unlike [^{3}H]-D-aspartate autoradiography, all 3 antibodies produced a distinct radial immunoreactivity pattern in white matter at all cord levels examined.

Autoradiographic Comparisons

In rat spinal cord, as in rat brain (26), EAAT2/GLT1 appeared to constitute a significant proportion of total EAAT distribution. Furthermore, spinal cord EAAT2/GLT1 binding density may be even greater than apparent in the current study because of the addition of KA to the assay buffer. KA and other glutamate agonists were added to block potential [^{3}H]-D-aspartate binding to glutamate receptors, but KA also inhibits EAAT2/GLT1, with negligible effect on EAAT1/GLAST and EAAT3/EAAC1 (27). That the apparent binding density of EAAT2/GLT1 could decrease in the presence of KA cannot be ruled out, but KA displacement of binding to EAAT1/GLAST and EAAT3/EAAC1 is unlikely. It is also possible that [^{3}H]-D-aspartate binding was below the threshold of detection in white matter by the same KA mechanism. White matter absorption of the low-energy beta emissions from tritium may also have limited [^{3}H]-D-aspartate detection in that tissue (43).

Differences in the observed levels of inhibition of EAAT2/GLT1 by DHK and 2,3-PDC on [^{3}H]-D-aspartate binding in rat cervical spinal cord are of particular interest. Although the available glutamate transport inhibitors do not absolutely delineate between all EAAT subtypes, both of these nontransportable inhibitors more potently inhibit EAAT2/GLT1 than EAAT1/GLAST or EAAT3/EAAC1 (42). DHK inhibited [^{3}H]-D-aspartate binding in dorsal and ventral cervical cord by an average of 12%, compared to an average of 40% inhibition by 2,3-PDC (Figure 2). The inhibition by DHK is similar to the 10% inhibition reported in rat brain. These different inhibitory profiles between brain and spinal cord and within spinal cord suggest that, in vivo, the potency of an inhibitor (particularly DHK) may not be as great as predicted from in vitro data and may reflect a cell, tissue, or regional dependency (18). For example, the neuronal EAAT2/GLT1 splice variant has been reported to exhibit a higher Ki for DHK than the originally described astrocytic GLT1 (44). If the splice variant accounts for a larger proportion of [^{3}H]-D-aspartate binding sites in cervical cord and brain than in thoracic and lumbar spinal cord (12,29–31), then DHK concentrations in the assay may not have been saturating against the neuronal variant. Qualitative immunohistochemistry results with GLT1 antibody also support this hypothesis, in that the most intense EAAT2/GLT1 immunoreactivity occurred in cervical spinal cord (Figure 3).

An important motive to measure Na^+-dependent transporter density is to determine the extent to which glutamate transporters bind glutamate and shape the postsynaptic signal, which is hypothesized to reflect the ratio of glutamate receptors to transporters in close proximity (36–39). To our knowledge, quantitative values of glutamate receptor binding density beyond ventral horn NMDA binding density (cord level unspecified) (45) in rat spinal cord have not been reported. A prior study of [^{3}H]-L-glutamate binding to rat spinal cord sections (46) would not have limited binding solely to glutamate receptors. It is difficult to reliably speculate on the role of glutamate transporters with respect to shaping rat spinal cord postsynaptic signals until studies are conducted with comparable experimental parameters. However, binding density has been quantified for spinal cord glutamate receptors and Na^+-dependent transporters in cat (47) and in human postmortem tissue (48–50). The ratio of receptor to transporter binding densities in both cat and human cord regions would indicate that the transporters more likely shape the postsynaptic signal in the dorsal and ventral horn.

Differences in experimental protocols should also be considered as a potential explanation for the observed variations in transporter distributions among the cat, human, and rat models. Compared to the [^{3}H]-D-aspartate binding density in cat (47), Na^+-dependent transporter density in rat spinal cord is approximately 10-fold lower. [^{3}H]-D-Aspartate distribution also differed between the 2 species in that binding density appeared greater in ventral than in dorsal horn in cat. However, the cat study was not conducted in the presence of glutamate receptor agonists or with a xylene pretreatment step, both of which affected binding density in the present study. Interestingly, Na^+-dependent transporter densities in human postmortem spinal cord tissue were greater in the dorsal horn (50), similar to the immunohistochemical results seen in the present study.

Compared to NMDA and non-NMDA glutamate receptor densities in rat spinal cord, the present autoradiography data suggest a more uniform distribution of EAATs throughout spinal cord gray matter, while glutamate receptors have a prominent distribution in the dorsal horn substantia gelatinosa (45,51,52). The measure scheme for the dorsal horn depicted in Figure 1, which included Rexed laminae I, II, III, and portions of IV (40,41), could mask significant differences in quantitative densities if measures had been taken in individual laminae. However, absolute densities of EAATs in the rat cord are approximately 10-fold lower than binding density in many brain regions (19), which implies a lower capacity to clear glutamate in spinal cord, assuming the majority of EAATs are plasma membrane bound (53–56). Although unlikely because of the time course involved, it cannot be ruled out that Na^+-dependent binding density was altered by decapitation. Sacrifice of rats by rapid cervical decapitation without anesthesia induces spinal convulsions, mediated in part by release of noradrenaline (57). Assuming simultaneous release of other neurotransmitters because of decapitation-induced depolarization and/or removal of descending inhibition, an acute increase in glutamate release might affect plasma membrane EAAT expression, such as reported with EAAT1/GLAST (58). The possible contribution of this phenomenon to reported EAAT binding density will be the subject of future experiments.

Immunohistochemistry Comparisons

Immunohistochemical regional labeling patterns with the 3 antibodies substantiated the results of prior immunoreactivity studies in spinal gray matter, which were conducted primarily in cervical cord tissue. Differences in experimental protocols could account for subtle differences in results. Our findings indicated immunoreactivity of EAAT2/GLT1 and EAAT1/GLAST most distinctly in laminae II, with laminae I clearly labeled only by EAAT3/EAAC1 antibody. Previous reports indicated immunoreactivity with antibodies to all 3 rat Na^+-dependent transporters in cervical dorsal horn laminae I–III (23) or I–II (25,35). The present results also indicated moderate to heavy EAAT2/GLT1 immunoreactivity in thoracic cord, in contrast to a report of slight thoracic GLT1 immunoreactivity by Vera-Portocarrero et al (35). The intense ventral horn motor neuronal immunoreactivity to EAAT3/EAAC1 antibody is consistent with that reported by Rothstein et al (23) and Vera-Portocarrero et al (35). Rothstein et al (23) also found moderate ventral horn labeling with GLAST, which was faintly apparent in the present study.

The importance of the EAAT system in spinal cord white matter is emphasized by (a) the apparent contribution of reversed glutamate transport to excitotoxic-induced white matter apoptosis (11,59), and (b) the fact that glutamate transport inhibitors protect from or decrease white matter pathology (10,11). This confirms previous reports of EAAT immunoreactivity in cervical spinal cord white matter (11,23,60). The variable results of these studies appear to be at least partially dependent upon whether C- or N-terminus antibodies were used, which may also be influenced by the presence of a EAAT2/GLT1 splice variant (31).

C-terminus antibodies to EAAT1/GLAST (23) and EAAT2/GLT1 (60) showed immunoreactivity in or along white matter tracts. EAAT3/EAAC1 immunoreactivity (C-terminus antibody) was present and possibly associated with oligodendrocytes (61). N-terminus antibodies demonstrate EAAT2/GLT1 and EAAT1/GLAST immunoreactivity in dorsal column astrocytes and in the axoplasm of myelinated axons (11). Nonradioactive in situ hybridization detected EAAT3/EAAC1 mRNA associated with oligodendroglia (28) and EAAT1/GLAST (25) and EAAT2/GLT1 (60) associated with astrocytes in white matter tracts.

CONCLUSION

In summary, this study confirmed the heterogeneous anatomic distribution of Na^+-dependent glutamate transporters throughout cervical, thoracic, and lumbar spinal cord, with greater density in gray matter than white matter. Integration of autoradiographic and immunohistochemical data provided a more complete picture of EAAT subtype distribution and density in rat spinal cord. Autoradiography may be more indicative of functional protein, whereas immunohistochemistry provides the cellular resolution unavailable with autoradiography. Based upon the relative densities of transporters and receptors, autoradiographic quantification of glutamate transporter should also shed some light on the extent to which uptake may contribute to signal termination (36–39) and or excitotoxic protection (8,32) (see Chen and Swanson [15] and Heath and Shaw [62] for review). Overall, EAAT density is lower in spinal cord than in brain, which may have important implications of spinal cord vulnerability to excitotoxic events. The density and distribution differences should be kept in mind when evaluating results from a specific cord level or

region and using that information to infer similar processes at other cord levels.

ACKNOWLEDGMENT

The authors thank Mr R. Steven Carroll for technical assistance.

REFERENCES

1. Liaw WJ, Stephens RL Jr, Binns BC, et al. Spinal glutamate uptake is critical for maintaining normal sensory transmission in rat spinal cord. *Pain.* 2005;115:60–70.
2. Rekling JC, Funk GD, Bayliss DA, Dong XW, Feldman JL. Synaptic control of motoneuronal excitability. *Physiol Rev.* 2000;80:767–852.
3. Agrawal SK, Fehlings MG. Role of NMDA and non-NMDA ionotropic glutamate receptors in traumatic spinal cord axonal injury. *J Neurosci.* 1997;17:1055–1063.
4. Wrathall JR, Choiniere D, Teng YD. Dose-dependent reduction of tissue loss and functional impairment after spinal cord trauma with the AMPA/kainate antagonist NBQX. *J Neurosci.* 1994;14:6598–6607.
5. Attwell D, Barbour B, Szatkowski M. Nonvesicular release of neurotransmitter. *Neuron.* 1993;11:401–407.
6. Zerangue N, Kavanaugh MP. Flux coupling in a neuronal glutamate transporter. *Nature.* 1996;383:634–637.
7. Rothstein JD, Martin LJ, Kuncl RW. Decreased glutamate transport by the brain and spinal cord in amyotrophic lateral sclerosis. *N Engl J Med.* 1992;326:1464–1468.
8. Rothstein JD, Jin L, Dykes-Hoberg M, Kuncl RW. Chronic inhibition of glutamate uptake produces a model of slow neurotoxicity. *Proc Natl Acad Sci U S A.* 1993;90:6591–6595.
9. Boston-Howes W, Gibb SL, Williams EO, Pasinelli P, Brown RH Jr, Trotti D. Caspase-3 cleaves and inactivates the glutamate transporter EAAT2. *J Biol Chem.* 2006;281:14076–14084.
10. McAdoo DJ, Xu G, Robak G, Hughes MG, Price EM. Evidence that reversed glutamate uptake contributes significantly to glutamate release following experimental injury to the rat spinal cord. *Brain Res.* 2000;865:283–285.
11. Li S. Novel injury mechanism in anoxia and trauma of spinal cord white matter: glutamate release via reverse Na+ dependent glutamate transport. *J Neurosci.* 1999 Jul15;19(14): RC16.
12. Yi JH, Hazell AS. Excitotoxic mechanisms and the role of astrocytic glutamate transporters in traumatic brain injury. *Neurochem Int.* 2006;48:394–403.
13. Weng HR, Chen JH, Cata JP. Inhibition of glutamate uptake in the spinal cord induces hyperalgesia and increased responses of spinal dorsal horn neurons to peripheral afferent stimulation. *Neuroscience.* 2006;138:1351–1360.
14. Springer JE, Azbill RD, Mark RJ, Begley JG, Waeg G, Mattson MP. 4-hydroxynonenal, a lipid peroxidation product, rapidly accumulates following traumatic spinal cord injury and inhibits glutamate uptake. *J Neurochem.* 1997;68:2469–2476.
15. Chen Y, Swanson RA. Astrocytes and brain injury. *J Cereb Blood Flow Metab.* 2003;23:137–149.
16. Flott B, Seifert W. Characterization of glutamate uptake systems in astrocyte primary cultures from rat brain. *Glia.* 1991;4:293–304.
17. Nichols DG. The release and uptake of excitatory amino acids. *Trends Pharmacol Sci.* 1990;11:462–468.
18. Robinson MB, Dowd LA. Heterogeneity and functional properties of subtypes of sodium-dependent glutamate transporters in the mammalian central nervous system. *Adv Pharmacol.* 1997;37:69–115.
19. Anderson KJ, Monaghan DT, Bridges RJ, Tavoularis AL, Cotman CW. Autoradiographic characterization of putative excitatory amino acid transport sites. *Neuroscience.* 1990;38:311–322.
20. Anderson KJ, Sandler DL. Autoradiography of L-[3H]aspartate binding sites. *Life Sci.* 1993;52:863–868.
21. Balcar VJ, Li Y, Killinger S. Effects of L-trans-pyrrolidine-2,4-dicarboxylate and L-threo-3-hydroxyaspartate on the binding of [3H]L-aspartate, [3H]alpha-amino-3-hydroxy-5-methyl-4-isoxazolepropionate (AMPA), [3H]DL-(E)-2-amino-4-propyl-5-phosphono-3-pentenoate (CGP 39653), [3H]6-cyano-7-nitroquinoxaline-2,3-dione (CNQX) and [3H]kainate studied by autoradiography in rat forebrain. *Neurochem Int.* 1995;26:155–164.
22. Levy LM, Lehre KP, Rolstad B, Danbolt NC. A monoclonal antibody raised against an [$Na^{++}K^{+}$]coupled L-glutamate transporter purified from rat brain confirms glial cell localization. *FEBS Lett.* 1993;317:79–84.
23. Rothstein JD, Martin L, Levey AI, et al. Localization of neuronal and glial glutamate transporters. *Neuron.* 1994;13:713–725.
24. Furuta A, Martin LJ, Lin CL, Dykes-Hoberg M, Rothstein JD. Cellular and synaptic localization of the neuronal glutamate transporters excitatory amino acid transporter 3 and 4. *Neuroscience.* 1997;81:1031–1042.
25. Schmitt A, Asan E, Puschel B, Kugler P. Cellular and regional distribution of the glutamate transporter GLAST in the CNS of rats: nonradioactive in situ hybridization and comparative immunocytochemistry. *J Neurosci.* 1997;17:1–10.
26. Danbolt NC. Glutamate uptake. *Prog Neurobiol.* 2001;65:1–105.
27. Arriza JL, Fairman WA, Wadiche JI, Murdoch GH, Kavanaugh MP, Amara SG. Functional comparisons of three glutamate transporter subtypes cloned from human motor cortex. *J Neurosci.* 1994;14:5559–5569.
28. Kugler P, Schmitt A. Glutamate transporter EAAC1 is expressed in neurons and glial cells in the rat nervous system. *Glia.* 1999;27:129–142.
29. Chen W, Aoki C, Mahadomrongkul V, et al. Expression of a variant form of the glutamate transporter GLT1 in neuronal cultures and in neurons and astrocytes in the rat brain. *J Neurosci.* 2002;22:2142–2152.
30. Schmitt A, Asan E, Lesch KP, Kugler P. A splice variant of glutamate transporter GLT1/EAAT2 expressed in neurons: cloning and localization in rat nervous system. *Neuroscience.* 2002;109:45–61.
31. Sullivan R, Rauen T, Fischer F, et al. Cloning, transport properties, and differential localization of two splice variants of GLT-1 in the rat CNS: implications for CNS glutamate homeostasis. *Glia.* 2004;45:155–169.
32. Rothstein JD, Dykes-Hoberg M, Pardo CA, et al. Knockout of glutamate transporters reveals a major role for astroglial transport in excitotoxicity and clearance of glutamate. *Neuron.* 1996;16:675–686.

33. Fairman WA, Vandenberg RJ, Arriza JL, Kavanaugh MP, Amara SG. An excitatory amino-acid transporter with properties of a ligand-gated chloride channel. *Nature.* 1995;375:599–603.
34. Arriza JL, Eliasof S, Kavanaugh MP, Amara SG. Excitatory amino acid transporter 5, a retinal glutamate transporter coupled to a chloride conductance. *Proc Natl Acad Sci U S A.* 1997;94:4155–4160.
35. Vera-Portocarrero LP, Mills CD, Ye Z, et al. Rapid changes in expression of glutamate transporters after spinal cord injury. *Brain Res.* 2002;927:104–110.
36. Bridges RJ, Esslinger CS. The excitatory amino acid transporters: pharmacological insights on substrate and inhibitor specificity of the EAAT subtypes. *Pharmacol Ther.* 2005;107:271–285.
37. Diamond JS, Jahr CE. Transporters buffer synaptically released glutamate on a submillisecond time scale. *J Neurosci.* 1997;17:4672–4687.
38. Tong G, Jahr CE. Block of glutamate transporters potentiates postsynaptic excitation. *Neuron.* 1994;13:1195–1203.
39. Wadiche JI, Arriza JL, Amara SG, Kavanaugh MP. Kinetics of a human glutamate transporter. *Neuron.* 1995;14:1019–1027.
40. Molander C, Xu Q, Grant G. The cytoarchitectonic organization of the spinal cord in the rat. I. The lower thoracic and lumbosacral cord. *J Comp Neurol.* 1984;230:133–141.
41. Molander C, Xu Q, Rivero-Melian C, Grant G. Cytoarchitectonic organization of the spinal cord in the rat: II. The cervical and upper thoracic cord. *J Comp Neurol.* 1989;289:375–385.
42. Bridges RJ, Kavanaugh MP, Chamberlin AR. A pharmacological review of competitive inhibitors and substrates of high-affinity, sodium-dependent glutamate transport in the central nervous system. *Curr Pharm Des.* 1999;5:363–379.
43. Kuhar MJ, De Souza EB, Unnerstall JR. Neurotransmitter receptor mapping by autoradiography and other methods. *Ann Rev Neurosci.* 1986;9:27–59.
44. Wang GJ, Chung HJ, Schnuer J, et al. High-affinity glutamate transport in rat cortical neurons in culture. *Mol Pharmacol.* 1998;53:88–96.
45. Monaghan DT, Cotman CW. Distribution of N-methyl-D-aspartate-sensitive L-[3H]glutamate-binding sites in rat brain. *J Neurosci.* 1985;5:2909–2919.
46. Greenamyre JT, Young AB, Penney JB. Quantitative autoradiographic distribution of L-[3H]glutamate-binding sites in rat central nervous system. *J Neurosci.* 1984;4:2133–2144.
47. Mitchell JJ, Anderson KJ. Quantitative autoradiographic analysis of excitatory amino acid receptors in the cat spinal cord. *Neurosci Lett.* 1991;124:269–272.
48. Shaw PJ, Ince PG, Johnson M, Perry EK, Candy J. The quantitative autoradiographic distribution of [3H]MK-801 binding sites in the normal human spinal cord. *Brain Res.* 1991;539:164–168.
49. Shaw PJ, Chinnery RM, Ince PG. Non-NMDA receptors in motor neuron disease (MND): a quantitative autoradiographic study in spinal cord and motor cortex using [3H]CNQX and [3H]kainate. *Brain Res.* 1994;655:186–194.
50. Shaw PJ, Chinnery RM, Ince PG. [3H]D-aspartate binding sites in the normal human spinal cord and changes in motor neuron disease: a quantitative autoradiographic study. *Brain Res.* 1994;655:195–201.
51. Monaghan DT, Cotman CW. The distribution of [3H]kainic acid binding sites in rat CNS as determined by autoradiography. *Brain Res.* 1982;252:91–100.
52. Henley JM, Jenkins R, Hunt SP. Localisation of glutamate receptor binding sites and mRNAs to the dorsal horn of the rat spinal cord. *Neuropharmacology.* 1993;32:37–41.
53. Davis KE, Straff DJ, Weinstein EA, et al. Multiple signaling pathways regulate cell surface expression and activity of the excitatory amino acid carrier 1 subtype of Glu transporter in C6 glioma. *J Neurosci.* 1998;18:2475–2485.
54. Duan S, Anderson CM, Stein BA, Swanson RA. Glutamate induces rapid upregulation of astrocyte glutamate transport and cell-surface expression of GLAST. *J Neurosci.* 1999;19:10193–10200.
55. Ikegaya Y, Matsuura S, Ueno S, et al. Beta-amyloid enhances glial glutamate uptake activity and attenuates synaptic efficacy. *J Biol Chem.* 2002;277:32180–32186.
56. Levenson J, Weeber E, Selcher JC, Kategaya LS, Sweatt JD, Eskin A. Long-term potentiation and contextual fear conditioning increase neuronal glutamate uptake. *Nat Neurosci.* 2002;5:155–161.
57. Roberts DC, Mason ST, Fibiger HC. Selective depletion of spinal noradrenaline abolishes post-decapitation convulsions. *Life Sci.* 1978;23:2411–2413.
58. Robinson MB. Regulated trafficking of neurotransmitter transporters: common notes but different melodies. *J Neurochem.* 2002;80:1–11.
59. Hassel B, Boldingh KA, Narvesen C, Iversen EG, Skrede KK. Glutamate transport, glutamine synthetase and phosphate-activated glutaminase in rat CNS white matter. A quantitative study. *J Neurochem.* 2003;87:230–237.
60. Schmitt A, Asan E, Puschel B, Jons T, Kugler P. Expression of the glutamate transporter GLT1 in neural cells of the rat central nervous system: non-radioactive in situ hybridization and comparative immunocytochemistry. *Neuroscience.* 1996;71:989–1004.
61. Kugler P, Schmitt A. Complementary neuronal and glial expression of two high-affinity glutamate transporter GLT1/EAAT2 forms in rat cerebral cortex. *Histochem Cell Biol.* 2003;119:425–435. Epub 2003 May 20.
62. Heath PR, Shaw PJ. Update on the glutamatergic neurotransmitter system and the role of excitotoxicity in amyotrophic lateral sclerosis. *Muscle Nerve.* 2002;26:438–458.